Grating-bicoupled plasmon-resonant terahertz emitter fabricated with GaAs-based heterostructure material systems

Taiichi Otsuji,[a] Yahya Moubarak Meziani, Mitsuhiro Hanabe, Takuma Ishibashi, and Tomohiro Uno
Research Institute of Electrical Communication, Tohoku University, 2-1-1 Katahira, Aoba-ku, Sendai 980-8577, Japan

Eiichi Sano
Research Center for Integrated Quantum Electronics, Hokkaido University, Nishi 8, Kita 13-Jo, Kita-ku, Sapporo, Hokkaido 060-8628, Japan

(Received 7 September 2006; accepted 16 November 2006; published online 26 December 2006)

A grating-bicoupled plasmon-resonant terahertz emitter was fabricated using InGaP/InGaAs/GaAs heterostructure material systems. The device structure is based on a high-electron mobility transistor and incorporates doubly interdigitated grating gates that periodically localize the two-dimensional (2D) plasmon in 100 nm regions with a submicron interval. Photoexcited electrons, injected to the 2D plasmon cavities, extensively promoted the plasmon instability, resulting in observation of emission of terahertz electromagnetic radiation at room temperature. © *2006 American Institute of Physics*. [DOI: 10.1063/1.2410228]

Two-dimensional (2D) plasmons in semiconductor heterostructures have attracted much attention due to their nature of instability promoting extraordinary electromagnetic radiation in the terahertz range, which is expected to realize frequency-tunable emitters as well as frequency multipliers.[1–8] Those previous works except Ref. 6 utilized dc-driven plasmon instability for emission of terahertz or subterahertz radiation, showing broad emission spectra even at cryogenic temperature. This is because electrical dc flow may excite various structure-dependent plasmon modes including gated and ungated regions.[7–9] Sekine *et al.* in Ref. 6 observed clear emission peak spectrum of terahertz radiation stimulated by impulsive Ti:sapphire laser excitation at cryogenic temperature, suggesting possibility of focused excitation of specific plasmon modes. So far, for this reason, a mean of terahertz emission/detection utilizing plasmon-resonant terahertz photomixing has been investigated.[9–15]

2D plasmon itself is a nonradiative mode so that a metal-wired grating coupler structure is frequently utilized to yield terahertz electromagnetic-wave emission.[1,2,5,6,13–15] Wilkinson *et al.* studied far-infrared response of plasmon excitation from biperiodically modulated 2D electron gas coupled with doubly interdigitated grating gates.[2] We have recently proposed a terahertz photomixer device incorporating similar grating-bicoupled periodic plasmon-resonant structure.[13] This letter reports on the observation of terahertz emission of radiation at room temperature stimulated by photoinduced 2D plasmon instability in a grating-bicoupled plasmon-resonant terahertz emitter fabricated with GaAs-based heterostructure material systems.

Figure 1 illustrates the cross section and plan view of the grating-bicoupled plasmon-resonant terahertz emitter. The device structure is based on a high-electron mobility transistor (HEMT) and incorporates doubly interdigitated grating gates (G1 and G2) that periodically localize the 2D plasmon in 100 nm regions with a submicron interval. The 2D plasmon layer is formed with a quantum well at the heterointerface between a 15-nm-thick undoped InGaAs channel layer and a 60-nm-thick, Si-δ doped InGaP carrier-supplying layer. According to the objective frequency band from 1 to 10 THz, the grating gate geometry was designed to have a length for a G1 (G2) finger: L_{G1} (L_{G2}) of 300 nm (100 nm) with a 100 nm space. The grating gate was formed with 65 -nm-thick Ti/Au/Ti by a standard lift-off process. When one group of the plasmon cavities under one gate grating (for example, G1) is charged with an appropriate 2D electronic density of 10^{11}–10^{12} cm^{-2} while the regions under another gate grating (for example, G2) are lightly charged with less 2D electron density by orders of magnitude, a strong electric field of the order of 1–10 kV/cm arises at the plasmon cavity boundaries. When the device is photoexcited by laser irradiation, photoelectrons are predominantly generated in the regions under G2 and then are injected to the plasmon cavities under G1. If a specific drain-to-source bias potential is applied to promote a potential slope along the source-to-drain direction on the energy band, photoelectrons in each depleted region under G2 are mainly injected to one side of the adjacent plasmon cavity under G1. This may lead to the excitation of plasmon instability. It is noted that the photo-

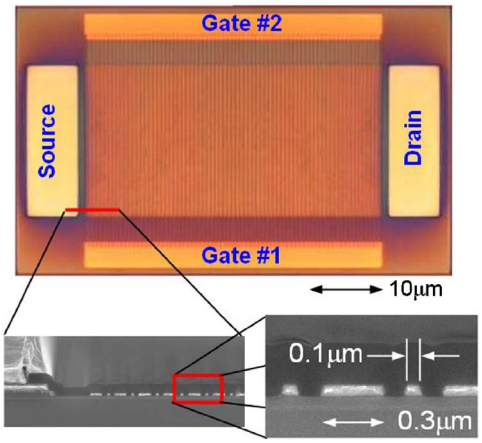

FIG. 1. (Color online) Device cross section and plan view.

[a]Electronic mail: otsuji@riec.tohoku.ac.jp

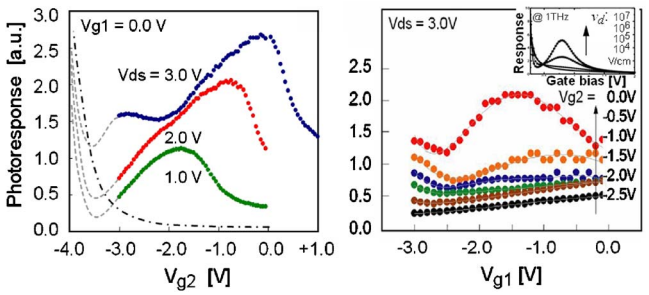

FIG. 2. (Color online) Measured photoresponse showing excitation of plasmon instability. (a) V_{g2} dependence and (b) V_{g1} dependence. The inset in (b) shows simulated photoresponse to a 100 nm gate HEMT under 1 THz radiation for different electron mobilities.

excitation may promote the plasmon instability in both regions under G1 and G2 if the cavity size and carrier density of those regions satisfy the resonant conditions.

According to the Mikhailov formulas[5] for the conditions of amplification of far-infrared radiation by means of dc-driven instability of grating-coupled 2D plasmons, the threshold velocity is still too high to perform room-temperature operation where electron drift mobility of the order of 10^5 $cm^2/(V\,s)$ is required even for idealistic III-V material systems. The periodically confined 2D plasmon grating structure of our proposal is expected to accelerate the instability leading to room-temperature operation. It is noted that the feature size of the grating is by two orders of magnitude smaller than the wavelength of terahertz electromagnetic waves under consideration.

Field emission properties of the device are characterized by the plasmon characteristic frequencies. The primary parameter is the plasma frequency ω_{p1} of the periodically confined *gated* plasmon cavities. Adding to ω_{p1}, the connecting portion (depleted regions under G2) as well as the gate metal gratings have their own characteristic frequencies, ω_{p2} and $\omega_{pm1,2}$, respectively.[13,14] Note that $\omega_{p1,2}$ for the gated plasmon cavities and connecting portions obey the linear dispersion law $\omega_{p1,2} \approx \sqrt{(e^2 d n_{1,2}/\varepsilon m^*)} i k_{G1,2}/2$, while $\omega_{pm1,2}$ for the *ungated* metallic regions is proportional to the square root of wave vector:[3–5] $\omega_{pm1,2} \approx \sqrt{i e^2 n_m k_{G1,2}/2\varepsilon m^*}$, where e is the elementary charge, d is the distance between the gate gratings and the plasmon gratings, $n_{1,2}$ is the 2D electron density at the plasmon cavities under G1 or G2, ε is the permittivity, m^* is the electron effective mass, i is a harmonic number, $k_{G1,2}$ is the wave number at the G1 or G2 region, and n_m is the surface electron density of the gate metal. Assuming those dispersion relations and device feature sizes, finite-differential time-domain simulation results in broadband terahertz emission produced by photoexcited plasmon instability.[13,14]

First, dc characteristics of the fabricated sample were measured. The drain current I_{ds} showed field-effect-transistor-like dependence on the drain-source bias V_{ds}, and the 2D electron density in the channel was successfully modulated by the dual gate bias V_{g1} and V_{g2} independently. Equivalent threshold voltage, $V_{th}=V_{g1}=V_{g2}$, was $V_{th} \approx -3.0$ V. Next, the device was irradiated from the backside with a 1.5 μm cw laser source to measure its photoresponse at room temperature. As shown in Figs. 2(a) and 2(b), the device exhibited an extraordinary photoresponse with relatively sharp peaks on its V_{g2} dependence and with a broad peak on its V_{g1} dependence. In particular, when $V_{ds}=3.0$ V as shown in Fig. 2(a), the photoresponse exhibited double peaks at $V_{g2}=0$ and -2.8 V corresponding to the fundamental and second-harmonic plasmon resonance, respectively. The results are completely different from that for standard HEMT devices fabricated on the same wafer showing monotonic dependence on the gate bias [plotted with a broken line in Fig. 2(a)].

The inset in Fig. 2(b) shows calculated photoresponse for a 100 nm gate HEMT under 1 THz radiation. If the device is excited with terahertz radiation, well-obtainable electron velocity below 10^7 V/cm can promote the plasmon resonance exhibiting similar peaky photoresponse, but in our case of dc driven excitation the threshold becomes high. Theoretical investigations in Refs. 5 and 16 suggest that the plasma instability is promoted when electrons have a very high drift velocity of around 4×10^7 cm/s (equivalent plasma-wave Mach number of around 0.5), which is reasonably obtained for injected photoelectrons at the plasmon cavity boundaries in our device. It is inferred, from such a phenomenological coincidence, that the unprecedented photoresponse of this work is attributed to the extraordinary plasmon excitation due to the injection of photoelectrons accelerated by the strong electric field arisen at the plasmon cavity boundaries, leading to emission of terahertz electromagnetic radiation.

In order to verify the emission of electromagnetic radiation from the device due to photoinduced plasmon instability, temporal electromagnetic response to impulsive photoexcitation was measured at room temperature by using a reflective electro-optic sampling system.[17] A 1.5 μm, fiber laser pulse with a 70 fs full width at half maximum and a 20 MHz repetition was used as pump and probe beams. The linearly polarized pump beam illuminated the device from the back surface. A CdTe electro-optic sensor crystal with Si prism was put on the sample. The probe beam, roughly cross polarized to the pump beam, was led to the sensor normal to the prism surface, which is fully reflected at the CdTe surface back to the electro-optic detection block. The reflective index tensor is modulated in proportion to the electric field arisen at the surface so that the time-resolved electric field along with the channel axis is detected as polarization change of the probe beam. The system bandwidth is expected to be over 4 THz, which is mainly limited by the optical phonon modes in the CdTe sensor crystal.[18]

First, as a reference, the measurement was done for a standard HEMT sample. The result showed a monotonic frequency response corresponding to a normal photoconductivity. Next, the sample was switched to the photomixer and biased at $V_{g1}=0.0$ V ($V_{th}+3.0$ V), $V_{g2}=-2.5$ V ($V_{th}+0.5$ V), and $V_{ds}=3.0$ V, close to the second-harmonic resonant point shown in Fig. 2(a). Typical measured impulse response and its Fourier transformed spectrum are shown in the upper right plot in Fig. 3. The Fourier spectrum exhibits resonant-like peaks over a wide frequency range from 800 GHz up to 4 THz, demonstrating emission of terahertz electromagnetic radiation. In particular, it is inferred that the spectral peaks at 900 GHz and its harmonic frequencies (1.8, 2.7, and 3.6 THz), designated with solid arrows in Fig. 3, are originated from the plasmon modes excited in the plasmon cavities under the G1 gates. The other subset of residual peaks at 750 GHz and its harmonic frequencies (1.5, 2.25, 3.0, and 3.75 THz), designated with open arrows in Fig. 3, are originated from the plasmon modes weakly excited in the plas-

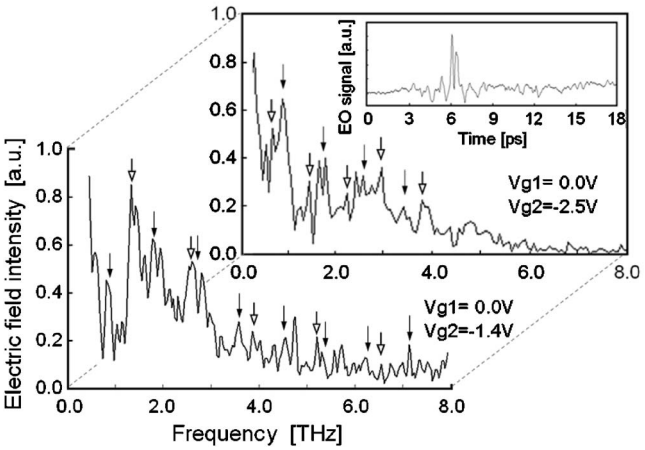

FIG. 3. Measured field emission spectrum when a 1.5 μm, 70 fs laser pulse is irradiated to the device. Upper right: $V_{g1}=0.0$ V, $V_{g2}=-2.5$ V, and $V_{ds}=3.0$ V; inset: temporal response of E_x; lower left: $V_{g1}=0.0$ V, $V_{g2}=-1.4$ V, and $V_{ds}=3.0$ V. Solid (open) arrows indicate possible plasmon modes for the cavities under G1 (G2).

mon cavities under the G2 gates. This is because the electron density in the regions under G1 is higher by almost one order of magnitude than that in the regions under G2 while the cavity size of the regions under G1 is three times larger than those under G2 so that the plasmon-resonant frequencies among them becomes in close proximity.

When V_{g2} was increased from -2.5 to -1.4 V ($V_{th}+1.6$ V) and other bias conditions were maintained, the original emission peaks at 750 GHz and its harmonics shifted up at 1.3 THz and its harmonics with higher intensity, while the other subset of emission peaks at 900 GHz and its harmonics were remained at the same points. (See the lower left plot in Fig. 3.) The estimated densities of electrons in the cavities under G2 are 7.4×10^{11} and 2.4×10^{12} cm^{-2} for V_{g2} of -2.5 and -1.4 V, respectively. Taking account of the Drude permittivity for those carrier densities, the observed emission spectrum well traces the 2D plasmon dispersion relations.

A grating-bicoupled plasmon-resonant terahertz emitter was fabricated using GaAs-based heterostructure material systems. Photoexcited electrons, injected to the 2D plasmon cavities, promoted the plasmon instability, resulting in observation of terahertz emission at room temperature.

The authors thank M. Dyakonov, V. Ryzhii, S. Mikhailov, and T. Asano for their valuable discussion and T. Nagatsuma for his supporting electro-optic sampling instrumentation. This work was financially supported in part by the SCOPE program from the MIC, Japan and by the Grant in Aid for Scientific Research (S) from the JSPS, Japan.

[1] D. C. Tsui, E. Gornik, and R. A. Logan, Solid State Commun. **35**, 875 (1980).
[2] R. J. Wilkinson, C. D. Ager, T. Duffield, H. P. Hughes, D. G. Hasko, H. Armed, J. E. F. Frost, D. C. Peacock, D. A. Ritchie, A. C. Jones, C. R. Whitehouse, and N. Apsley, J. Appl. Phys. **71**, 6049 (1992).
[3] M. Dyakonov and M. Shur, Phys. Rev. Lett. **71**, 2465 (1993).
[4] M. Dyakonov and M. Shur, IEEE Trans. Electron Devices **43**, 380 (1996).
[5] S. A. Mikhailov, Phys. Rev. B **58**, 1517 (1998).
[6] N. Sekine, K. Yamanaka, K. Hirakawa, M. Voseburger, P. Haring-Bolivar, and H. Kurz, Appl. Phys. Lett. **74**, 1006 (1999).
[7] W. Knap, J. Lusakowski, T. Parenty, S. Bollaert, A. Cappy, V. V. Popov, and M. S. Shur, Appl. Phys. Lett. **84**, 2331 (2004).
[8] N. Dyakonova, A. El Fatimy, J. Lusakowski, W. Knap, M. I. Dyakonov, M.-A. Poisson, E. Morvan, S. Bollaert, A. Shchepetov, Y. Roelens, Ch. Gaquiere, D. Theron, and A. Cappy, Appl. Phys. Lett. **88**, 141906 (2006).
[9] A. Satou, V. Ryshii, I. Khmyrova, M. Ryzhii, and M. S. Shur, J. Appl. Phys. **95**, 2048 (2004).
[10] T. Otsuji, S. Nakae, and H. Kitamura, IEICE Trans. Electron. **E84-C**, 1470 (2001).
[11] V. Ryzhii, I. Khmyrova, A. Satou, P. O. Vaccaro, T. Aida, and M. Shur, J. Appl. Phys. **92**, 5756 (2002).
[12] T. Otsuji, M. Hanabe, and O. Ogawara, Appl. Phys. Lett. **85**, 2119 (2004).
[13] T. Otsuji, M. Hanabe, T. Nishimura, and E. Sano, Opt. Express **14**, 4815 (2006).
[14] M. Hanabe, T. Nishimura, M. Miyamoto, T. Otsuji, and E. Sano, IEICE Trans. Electron. **E89-C**, 985 (2006).
[15] T. Nishimura, M. Hanabe, M. Miyamoto, T. Otsuji, and E. Sano, IEICE Trans. Electron. **E89-C**, 1005 (2006).
[16] V. Ryzhii, A. Satou, and M. S. Shur, IEICE Trans. Electron. **E89-C**, 1012 (2006).
[17] L. Min and R. J. D. Miller, Appl. Phys. Lett. **56**, 524 (1990).
[18] M. S. Kushwaha and S. S. Kushwaha, Can. J. Phys. **58**, 351 (1980).